Design of a compact and high sensitive refractive index sensor base on metal-insulator-metal plasmonic Bragg grating

Yun Binfeng, Hu Guohua, Zhang Ruohu and Cui Yiping*

Advanced Photonics Center, Southeast University, Nanjing, 210096 China
**cyp@seu.edu.cn*

Abstract: A nanometric and high sensitive refractive index sensor based on the metal-insulator-metal plasmonic Bragg grating is proposed. The wavelength encoded sensing characteristics of the refractive index sensor were investigated by analyzing its transmission spectrum. The numerical results show that a good linear relationship between the Bragg wavelength and the refractive index of the sensing material can be obtained, which is in accordance with the analytical results very well. A high refractive index sensitivity of 1488nm/RIU around Bragg resonance wavelength of 1550nm was obtained. Besides, the simulation results show that the sensitivity is depended on the Bragg resonance wavelength and the longer the Bragg resonance wavelength, the higher sensitivity can be obtained. Furthermore, the figure of merit of the refractive index sensor can be greatly increased by introducing a nano-cavity in the proposed plasmonic Bragg grating structure. This work pave the way for high sensitive nanometric refractive index sensor design and application.

OCIS codes: (240.6680) Surface plasmons; (310.6628) Subwavelength structures, nanostructures; (280.4788) Optical sensing and sensors.

References and links

1. E. Ozbay, "Plasmonics: merging photonics and electronics at nanoscale dimensions," Science **311**(5758), 189–193 (2006).
2. S. S. Xiao, L. Liu, and M. Qiu, "Resonator channel drop filters in a plasmon-polaritons metal," Opt. Express **14**(7), 2932–2937 (2006).
3. B. F. Yun, G. H. Hu, and Y. P. Cui, "Theoretical analysis of a nanoscale plasmonic filter based on a rectangular metal-insulator-metal waveguide," J. Phys. D Appl. Phys. **43**(38), 385102 (2010).
4. X. S. Lin and X. G. Huang, "Tooth-shaped plasmonic waveguide filters with nanometeric sizes," Opt. Lett. **33**(23), 2874–2876 (2008).
5. Y. Matsuzaki, T. Okamoto, M. Haraguchi, M. Fukui, and M. Nakagaki, "Characteristics of gap plasmon waveguide with stub structures," Opt. Express **16**(21), 16314–16325 (2008).
6. Q. Zhang, X. G. Huang, X. S. Lin, J. Tao, and X. P. Jin, "A subwavelength coupler-type MIM optical filter," Opt. Express **17**(9), 7533–7549 (2009).
7. B. F. Yun, G. H. Hu, and Y. P. Cui, "A nanometric plasmonic waveguide filter based on Fabry-Perot resonator," Opt. Commun. **284**(1), 485–489 (2011).
8. J. Zhang, L. K. Cai, W. L. Bai, and G. F. Song, "Flat Surface Plasmon Polariton Bands in Bragg Grating Waveguide for Slow Light," J. Lightwave Technol. **28**(14), 2030–2036 (2010).
9. Y. F. Liu, Y. Liu, and J. Kim, "Characteristics of plasmonic Bragg reflectors with insulator width modulated in sawtooth profiles," Opt. Express **18**(11), 11589–11598 (2010).
10. A. Hossieni and Y. Massoud, "A low-loss metal-insulator-metal plasmonic bragg reflector," Opt. Express **14**(23), 11318–11323 (2006).
11. J. Q. Liu, L. L. Wang, M. D. He, W. Q. Huang, D. Y. Wang, B. S. Zou, and S. C. Wen, "A wide bandgap plasmonic Bragg reflector," Opt. Express **16**(7), 4888–4894 (2008).
12. A. Hosseini, H. Nejati, and Y. Massoud, "Modeling and design methodology for metal-insulator-metal plasmonic Bragg reflectors," Opt. Express **16**(3), 1475–1480 (2008).
13. C. Wu, G. Song, L. Yu, and J. H. Xiao, "Tunable narrow band filter based on a surface plasmon polaritons Bragg grating with a metal-insulator-metal waveguide," J. Mod. Opt. **60**(15), 1217–1222 (2013).
14. D. C. Zografopoulos and R. Beccherelli, "Liquid-crystal-tunable metal-insulator-metal plasmonic waveguides and Bragg resonators," J. Opt. **15**(5), 055009 (2013).

#223182 - $15.00 USD Received 15 Sep 2014; revised 19 Oct 2014; accepted 25 Oct 2014; published 10 Nov 2014

15. Y. J. Chang and C. Y. Chen, "Ultracompact, narrowband three-dimensional plasmonic waveguide Bragg grating in metal/multi-insulator/metal configuration," Appl. Opt. **52**(4), 889–896 (2013).
16. J. Xiao, J. S. Liu, Z. Zheng, Y. S. Bian, G. J. Wang, and S. N. Li, "Transmission performance of a low-loss metal-insulator-semiconductor plasmonic phase-shift Bragg grating," Phys. Status Solidi A **209**(8), 1552–1556 (2012).
17. Y. J. Chang, "Design and analysis of metal/multi-insulator/metal waveguide plasmonic Bragg grating," Opt. Express **18**(12), 13258–13270 (2010).
18. Y. J. Chang and G. Y. Lo, "A Narrowband Metal-Multi-Insulator-Metal Waveguide Plasmonic Bragg Grating," IEEE Photon. Technol. Lett. **22**(9), 634–636 (2010).
19. Y. K. Gong, X. M. Liu, and L. R. Wang, "High-channel-count plasmonic filter with the metal-insulator-metal Fibonacci-sequence gratings," Opt. Lett. **35**(3), 285–287 (2010).
20. Y. K. Gong, L. R. Wang, X. H. Hu, X. H. Li, and X. M. Liu, "Broad-bandgap and low-sidelobe surface plasmon polariton reflector with Bragg-grating-based MIM waveguide," Opt. Express **17**(16), 13727–13736 (2009).
21. J. Park, H. Kim, and B. Lee, "High order plasmonic Bragg reflection in the metal-insulator-metal waveguide Bragg grating," Opt. Express **16**(1), 413–425 (2008).
22. Y. X. Xiang, X. Z. Zhang, W. Cai, L. Wang, C. F. Ying, and J. J. Xu, "Optical bistability based on Bragg grating resonators in metal-insulator-metal plasmonic waveguides," AIP. Adv **3**, 12106 (2013).
23. N. Chen, B. F. Yun, and Y. P. Cui, "Cladding mode resonances of etch-eroded fiber Bragg grating for ambient refractive index sensing," Appl. Phys. Lett. **88**(13), 133902 (2006).
24. A. N. Chryssis, S. M. Lee, S. B. Lee, S. S. Saini, and M. Dagenais, "High sensitivity evanescent field fiber Bragg grating sensor," IEEE Photon. Technol. Lett. **17**(6), 1253–1255 (2005).
25. T. Wu, Y. Liu, Z. Yu, Y. Peng, C. Shu, and H. Ye, "The sensing characteristics of plasmonic waveguide with a ring resonator," Opt. Express **22**(7), 7669–7677 (2014).
26. T. Wu, Y. M. Liu, Z. Y. Yu, Y. W. Peng, C. G. Shu, and H. F. He, "The sensing characteristics of plasmonic waveguide with a single defect," Opt. Commun. **323**, 44–48 (2014).
27. M. Chamanzar, M. Soltani, B. Momeni, S. Yegnanarayanan, and A. Adibi, "Hybrid photonic surface-plasmon-polariton ring resonators for sensing applications," Appl. Phys. B **101**(1-2), 263–271 (2010).
28. D. C. Zografopoulos, E. E. Kriezis, B. Bellini, and R. Beccherelli, "Tunable one-dimensional photonic crystal slabs based on preferential etching of silicon-on-insulator," Opt. Express **15**(4), 1832–1844 (2007).
29. A. C. Tasolamprou, B. Bellini, D. C. Zografopoulos, E. E. Kriezis, and R. Beccherelli, "Tunable optical properties of silicon-on-insulator photonic crystal slab structures," J. Eur. Opt. Soc-Rapid **4**, 09017 (2009).
30. I. M. White and X. D. Fan, "On the performance quantification of resonant refractive index sensors," Opt. Express **16**(2), 1020–1028 (2008).
31. G. Gilardi and R. Beccherelli, "Integrated optics nano-opto-fluidic sensor based on whispering gallery modes for picoliter volume refractometry," J. Phys. D Appl. Phys. **46**(10), 105104 (2013).

1. Introduction

Surface plasmon polaritons (SPPs) are electromagnetic waves coherently coupled to electron oscillations which propagates at the interface between a dielectric and a metal, with evanescently decaying fields in both sides [1]. Until now, there are basically two kinds of SPP waveguide, one is the insulator-metal-insulator (IMI) SPP waveguide and the other is metal-insulator-metal (MIM) SPP waveguide. Comparing with large mode size (several micrometers) of IMI SPP waveguide, the MIM SPP waveguide can squeeze the mode size down to a few tens of nanometer, which is very promising for the nanoscale applications. So a lot of nano plasmonic filter structures such as ring resonator [2, 3], stub resonator [4, 5], Fabry-Perot resonator [6, 7], Bragg grating [8–22] and so on have been proposed. Among them, the plasmonic MIM Bragg grating can be realized by waveguide width modulation [8, 9], waveguide core refractive index modulation [10] and combination of them [11, 12]. Until now, almost all the plasmonic Bragg gratings have been proposed to be used in the optical communication fields such as the optical filters [13–21], optical bistablity [22] and slow light [8]. As we known, another important application for the waveguide Bragg grating is sensing because the Bragg wavelength can be modulated by the surrounding environments such as the strain, force, temperature and refractive index. The fiber Bragg grating (FBG) has been proposed as the refractive index sensor by reducing the cladding layer thickness. Using the fiber cladding modes, we demonstrated a FBG refractive index sensor with maximum sensitivity of 172nm/RIU by reducing the cladding thickness to about 20μm [23]. By even etching the fiber core down to 3μm, a FBG refractive index sensor with highest sensitivity of 1394nm/RIU has been reported [24]. There are several limitations for the FBG based refractive index sensors. First, due to the silica material of the fiber core, the maximum surrounding refractive index to be measured must below 1.45, otherwise no waveguide modes can be supported. So the refractive index sensing range is limited; Second, the relation

#223182 - $15.00 USD Received 15 Sep 2014; revised 19 Oct 2014; accepted 25 Oct 2014; published 10 Nov 2014

between the Bragg wavelength of the FBG and the surrounding refractive index is not linear (the refractive index sensitivity increases with increasing surrounding refractive index). This will increase the complexity of the sensor encoding and demodulation, which is not ideal for sensing applications; Third, reducing the cladding layer thickness and even down to the core region will make the fiber fragile and very easy to be broken, which will make the encapsulation difficult; Last, even etching to the fiber core, the FBG refractive sensor is still relative large (several micrometers in width and several millimeters in length). In order to overcome these limitations, here we proposed a compact (several tens of nanometers in width and several micrometers in length) and high sensitive refractive index sensor based on the MIM plasmonic Bragg grating. The refractive index sensing range in not limited because the fundamental MIM waveguide mode is not cutoff. And comparing with nonlinear response of the traditional dielectric waveguide refractive index sensor, a nearly linear relationship between the Bragg wavelength and the refractive index of the measurand can be obtained, which is caused by the different dispersion relations between the dielectric waveguides and the plasmonics MIM waveguides. The sensing characteristics of the proposed MIM plasmonic Bragg grating were analyzed in detail, which have not been investigated yet. The results show that the proposed MIM plasmonic Bragg grating can overcome the shortages of the FBG based refractive index sensor and are very promising for chemical and biological sensing.

2. Refractive index sensor based on MIM Bragg grating

The structure of the proposed refractive index sensor based on the MIM plasmonic Bragg grating is shown as Fig. 1, which is realized by periodic MIM waveguide width modulation. The w_1, w_2, d_1 and d_2 denote the widths and lengths of the two segments, which are repeated to form the periodic MIM Bragg grating. Here we choose silver as the metal and the MIM waveguide core is assumed to be filled with the material to be measured (refractive index of nc). The targeted measurand could be some kind of liquid solution or gas. The liquid filling can be achieved by capillary attraction. And the light can be coupled into the sensor by nano-fiber and the output light can be detected by JY Confocal Raman Microscopy [25, 26]. In the article, the solution (gas) is considered as transparent because the absorption of liquid solution (gas) is much less than the metal, the effect of liquid (gas) absorption is neglected. The fundamental TM mode supported in the MIM waveguide can be obtained by the following dispersion relation [7]:

$$\varepsilon_{in} k_{z2} + \varepsilon_m k_{z1} \coth\left(-\frac{ik_{z1}}{2} w\right) = 0 \tag{1}$$

and k_{z1} and k_{z2} are

$$k_{z1}^2 = \varepsilon_{in} k_0^2 - \beta^2, k_{z2}^2 = \varepsilon_m k_0^2 - \beta^2 \tag{2}$$

where $\varepsilon_{in}, \varepsilon_m$ are the dielectric constants of the insulator and the metal, $k_0 = 2\pi/\lambda$ is the free space wave vector. Here the dielectric constant of the silver is characterized by the well known Drude model [6]:

$$\varepsilon_m(\omega) = \varepsilon_\infty - \omega_p^2 / \omega(\omega + i\gamma) \tag{3}$$

where $\omega_p = 1.38 \times 10^{16} Hz$ is the bulk plasma frequency, which represents the nature frequency of the oscillations of free conduction electrons, $\gamma = 2.73 \times 10^{13} Hz$ is the damping frequency of the oscillations, ω is the angular frequency of the incident light, and $\varepsilon_\infty = 3.7$ is the dielectric constant at infinite angular frequency [6]. In order to investigate the characteristics of the proposed refractive index sensor, a commercial software package RSORT FullWAVE, which based on the finite difference time domain (FDTD) method with perfect matched layer boundary condition was used to obtain the transmission spectra of the 2D MIM Bragg grating.

#223182 - $15.00 USD Received 15 Sep 2014; revised 19 Oct 2014; accepted 25 Oct 2014; published 10 Nov 2014

The fundamental TM mode is excited by a pulse source and the mesh grid size is set to 1nm in order to keep convergence.

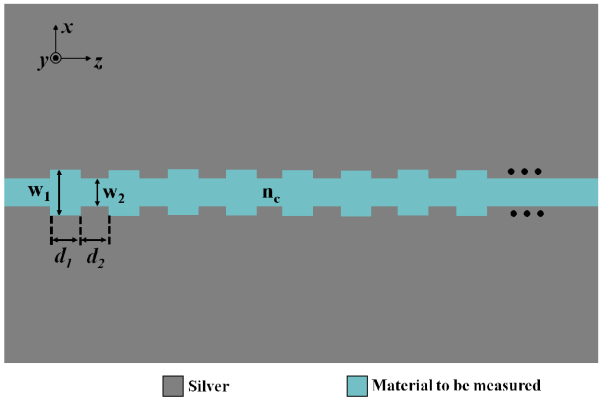

Fig. 1. The structure of the MIM plasmonic Bragg grating.

In order to optimize the proposed MIM plasmonic Bragg grating for sensing application, the structure parameter effects on the transmission spectra of the MIM plasmonic Bragg gratings were investigated. Figure 2(a) shows the transmission spectra of the MIM plasmonic Bragg gratings with different period numbers (N), while other parameters are fixed. It is obvious that the transmission dip gets deeper with increasing period number and the Bragg wavelength is almost unchanged, which is same as the FBG. But the total period number needed for MIM Bragg grating is much fewer than the FBG, this is because the effective index modulation strength of the MIM Bragg grating is much higher than the FBG, which can make the MIM Bragg grating much shorter than the FBG. From Fig. 2(a), we can see if there are too few periods, the transmission dip is shallow and may be difficult to measure while if the periods are too many, the bottom of transmission spectrum gets saturated and the Bragg wavelength at transmission dip is difficult to be distinguished. Although the linear scale can be changed to the logarithmic scale to enhance the dip resolution, there are two disadvantages by increasing periods: First, The device's total loss will be increased due to the strong metal absorption, and the Q factor will degrade if too much loss is introduced; Second, The device's size will be enlarged, which is not expectable for our compact sensor. So we can choose limited periods to construct the sensor as long as extinction ratio of the transmission dip is deep enough. Figure 2(b) shows the transmission spectra of the MIM plasmonic Bragg gratings with different duty cycles of width modulation, while keep the Bragg resonance wavelength fixed according to the following well-known Bragg condition [10]:

$$d_1 \times \mathrm{Re}\,al(\mathrm{n}_{\mathrm{eff}1}) + \mathrm{d}_2 \times \mathrm{Re}\,al(n_{eff\,2}) = \lambda_B / 2 \qquad (4)$$

Where n_{eff1} and n_{eff2} are the MIM waveguide mode effective indices of the wider and narrower segments of the MIM Bragg grating. The results show that the deepest dip can be obtained when the duty cycle of the width modulation equals 1:1. According to the above simulation results, we choose N = 10 and d_1:d_2 = 1:1 in the following MIM plasmonic Bragg grating refractive index sensor design.

#223182 - $15.00 USD Received 15 Sep 2014; revised 19 Oct 2014; accepted 25 Oct 2014; published 10 Nov 2014

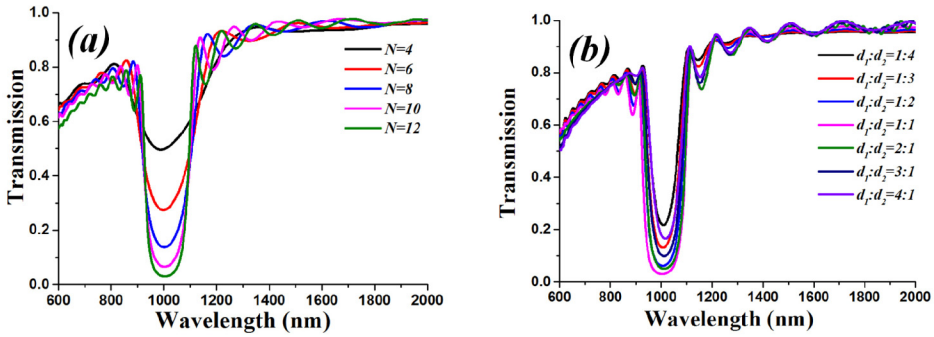

Fig. 2. (a) The transmission spectra of the MIM Bragg grating with different period numbers (w1 = 100nm,w2 = 80nm,n_c = 1,d1 = d2 = 202nm). (b) The transmission spectra of the MIM Bragg grating with different duty cycles of width modulation(w1 = 100nm,w2 = 80nm, n_c = 1, N = 12).

Then the sensing characteristics of the proposed MIM plasmonic Bragg grating were investigated by tracking the transmission dip when the refractive index of the material n_c was changed. The transmission spectra of the MIM Bragg grating with different refractive index n_c were simulated by using the FDTD method and shown in Fig. 3(a). When refractive index n_c was increased from 1 to 1.5, the transmission spectra were obviously red shifted and the Bragg resonance wavelength at the transmission dip was red shifted from 1000nm to 1504nm. By combing the dispersion relation Eq. (1) and the Bragg condition Eq. (4), the Bragg resonance wavelength versus the refractive index n_c was obtained analytically and shown as red line in Fig. 3(b). And a linear refractive index sensitivity of 1009nm/RIU was obtained. Also the relationship between the refractive index n_c and the Bragg resonance wavelength obtained by the numerical FDTD method is shown as dots in the Fig. 3(b), which is in accordance with the analytical results very well. In addition, the bandwidth of the MIM Bragg grating was increased when the refractive index n_c was increased. This is caused by the increasing mode effective refractive index modulation strength of the grating with increasing refractive index n_c according to the dispersion relation Eq. (1). As we know, the figure of merit (FOM), which is defined as the ratio of the wavelength sensitivity to the 3dB bandwidth of the transmission spectrum and often used to characterize the sensor performance [27]. From Fig. 3(a), due to the enlarged bandwidth of the transmission spectrum, the FOM of the MIM Bragg grating is reduced from 5.86 to 3.86 when the refractive index n_c increased from 1 to 1.5. Usually, silver is keen to tarnish when exposed to tiny quantities of ozone and H_2S present in air, which will degrade the sensor performance. So sensing characteristics of the gold MIM plasmonic Bragg grating with the same structure parameters are investigated too and the results are shown in Fig. 3(c), 3(d). Very similar sensing characteristics are obtained with a linear refractive index sensitivity of 1028 nm/RIU, and the FOM is reduced from 5.71 to 1.61 when the refractive index n_c increased from 1 to 1.5.

#223182 - $15.00 USD Received 15 Sep 2014; revised 19 Oct 2014; accepted 25 Oct 2014; published 10 Nov 2014

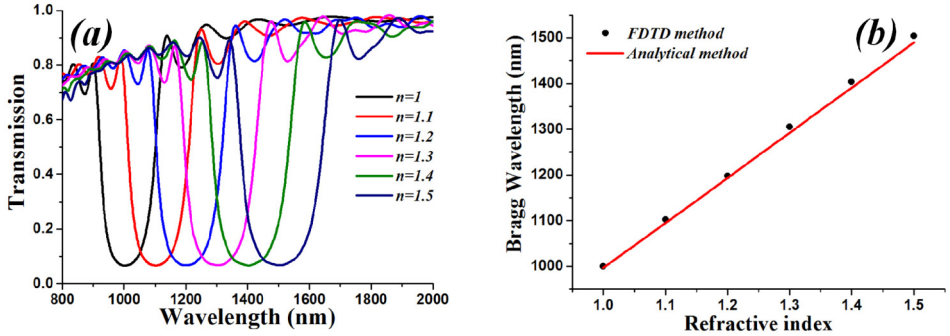

Fig. 3. (a, c) The transmission spectra of MIM Bragg grating with different refractive index n_c. (b, d) The Bragg resonance wavelength versus the refractive index (n_c) of the material under sensing (The MIM grating parameters are: w_1 = 100nm,w_2 = 80nm,d_1 = d_2 = 202nm,N = 10).

The realistic MIM Bragg grating refractive index sensor should be three dimensional and here we assume the structure is fabricated on the silicon dioxide substrate, which is shown as Fig. 4(a). The structure parameters of the MIM Bragg grating are w_1 = 100nm,w_2 = 80nm, h = 100 nm, d_1 = d_2 = 202nm, N = 10, and the refractive index of the silicon dioxide is taken as 1.44. The relationship between the refractive index of the measurand and the Bragg wavelength is simulated according to Eq. (4) and shown in Fig. 4(b). Similar linear response is obtained and the refractive index sensitivity obtained from Fig. 4(b) is about 650nm/RIU, which is lower than the two dimensional case in Fig. 3(a). This is because the height of the silver film is only 100nm, which is much thinner than in the infinite of the two dimensional case. The sensitivity can be enhanced by increasing the metal film thickness. Also the out of plane loss occurred in the three dimensional device should be considered, which is different from the two dimensional case [28, 29], but here the out of plane loss is neglected for simplicity because only the Bragg wavelength is need to be detected. The sensitivity of 650nm/RIU in our qusi-3D simulation is moderate in some representative refractive index sensors (such as SPR based, photonic crystal based, dielectric waveguide based) [30], but it has the nearly linear response, which is very desire for sensing application and cannot be achieved by most other refractive index sensors. The another advantage of the MIM Bragg grating sensor is that very litter fluid volume is needed according to it's nanometric size. The total size of the structure is on the order of 10μm × 100nm × 100nm = 0.1μm^3. So ideally only volume of 0.1fL is needed and if a 10μm thick layer of liquid is covered on the sensing region, the volume needed is just10fL, which leads to a sensitivity of 65nm/RIU/fL and is much higher than other refractive index sensor [31].

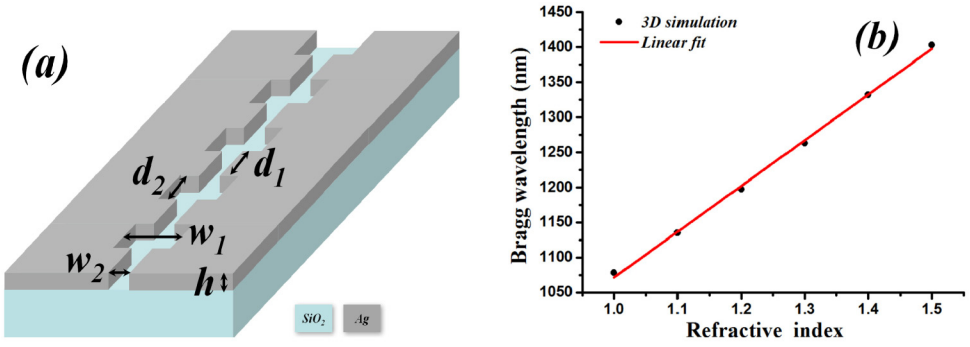

Fig. 4. (a) The schematic of the three dimensional MIM Bragg grating. (b) The Bragg resonance wavelength versus the refractive index (n_c) of the material under sensing (The 3D MIM grating parameters are: w_1 = 100nm,w_2 = 80nm, h = 100 nm, d_1 = d_2 = 202nm, N = 10).

#223182 - $15.00 USD Received 15 Sep 2014; revised 19 Oct 2014; accepted 25 Oct 2014; published 10 Nov 2014

In order to improve the sensitivity of the sensor, the structure parameters effects on the sensitivity were investigated. And for simplicity, following simulations are base on the two dimensional MIM Bragg gratings. First, refractive index sensitivities of MIM Bragg gratings with same Bragg wavelength were analyzed. According to the Bragg condition, three MIM Bragg grating(G_1, G_2, G_3) with same Bragg wavelength around 1000nm are realized by choosing different combinations of grating parameters. The obtained relationships between the Bragg resonance wavelengths and the refractive index n_c are shown in Fig. 5(a). The sensitivities of the three different MIM Bragg grating are 998nm/RIU, 1009nm/RIU and 1027nm/RIU, which are almost same. Then the sensitivities of the MIM Bragg gratings with different Bragg resonance wavelengths were investigated. Here we changed the Bragg resonance wavelength of the MIM Bragg grating by altering the grating period and keeping the other grating parameters unchanged. The obtained relationships between the Bragg resonance wavelengths and the refractive index n_c of three MIM Bragg gratings with different grating periods are shown in Fig. 5(b). The Bragg resonance wavelengths of the three MIM Bragg gratings are 999nm, 1296nm and 1486nm, and the refractive index sensitivities of them are 998nm/RIU, 1273nm/RIU and 1475nm/RIU, respectively. It is obvious that even higher refractive index sensitivity can be achieved by red shifting the Bragg resonance wavelength, which can be easily realized by increasing the grating period.

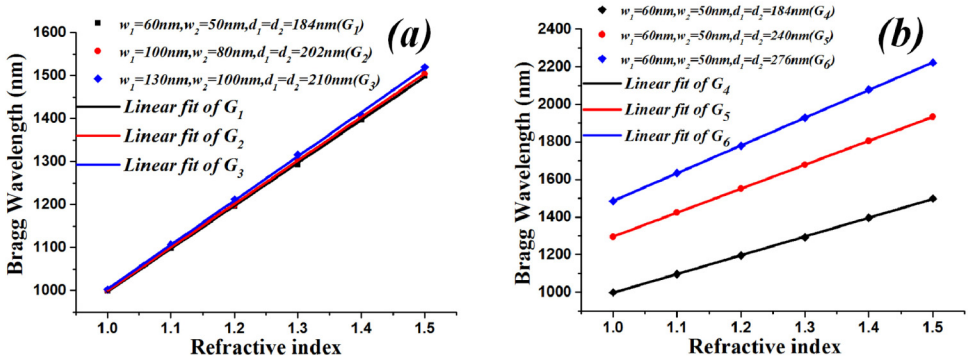

Fig. 5. (a) The Bragg resonance wavelengths versus the refractive index (n_c) of three different MIM Bragg gratings with same Bragg wavelength. (b) The Bragg resonance wavelengths versus the refractive index (n_c) of three MIM Bragg gratings with different grating periods (w_1 = 60nm,w_2 = 50nm,N = 10).

3. Improving FOM by using nano-cavity in MIM Bragg grating

From above investigation, a high sensitive refractive index sensor can be achieved by the MIM plasmonic Bragg grating but the FOM of the sensor is relative low, which is caused by the large bandwidth of the MIM plasmonic Bragg grating due to the relative large effective mode index modulation. It is well known that a narrow transmission peak can be formed in the transmission stop band by introducing a nano-cavity in the MIM plasmonic Bragg grating [10, 11]. Here we introducing a nano-cavity with length of $L_c = 2d_1 = 2d_2$ in the MIM plasmonic Bragg grating as shown in Fig. 6.

#223182 - $15.00 USD Received 15 Sep 2014; revised 19 Oct 2014; accepted 25 Oct 2014; published 10 Nov 2014

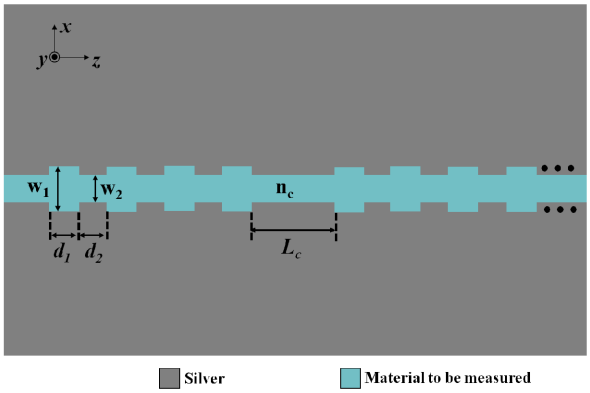

Fig. 6. The structure of the MIM plasmonic Bragg grating with nano-cavity.

The obtained transmission spectrum of the MIM Bragg grating with a nano-cavity in the center is shown as the solid red line in Fig. 7(a) and the transmission spectrum of the uniform MIM Bragg grating is also shown as black dotted line for comparison. It is obvious that a narrow transmission peak appears in the center of the rejection band as expected. At the resonance wavelength of 1003nm, the 3dB bandwidth of MIM Bragg grating with a nano-cavity is about 38nm, which is much narrower than the 172nm of uniform MIM Bragg grating. Using the sensitivity of 1009nm/RIU obtained above, the FOM is greatly increased from 5.86 to about 26.5. So the FOM of the refractive sensor can be increased by tracking the transmission peak of the MIM Bragg grating with a nano-cavity. Also same as the uniform MIM Bragg grating, the refractive index sensitivity of the MIM Bragg grating with a nano-cavity can be enhanced by increasing the grating period. Here we choose three samples with different grating periods (G_7, G_8, G_9) and the obtained peak resonance wavelengths versus the refractive index (nc) are shown in Fig. 7(b). The resonance wavelengths of G_7, G_8 and G_9 are 1003nm, 1298nm and 1490nm, respectively. The refractive index sensitivities are 983nm/RIU, 1286nm/RIU and 1488nm/RIU, respectively. And the corresponding FOMs are about 18.9, 22.2 and 19.8, respectively.

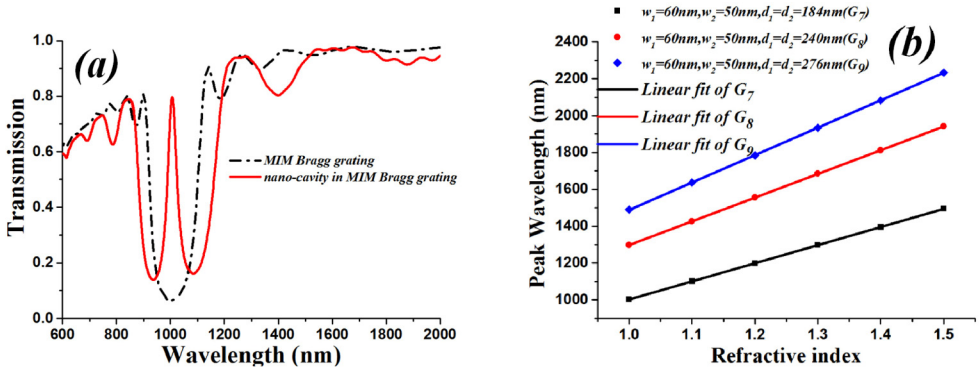

Fig. 7. (a) The transmission spectra of the MIM Bragg grating and the MIM Bragg grating with a nano-cavity in the center (w_1 = 100,w_2 = 80,d_1 = d_2 = 202, L_c = 2d_1 = 404, N = 10). (b) The peak resonance wavelengths versus the refractive index (n_c) of three MIM Bragg gratings with nano-cavities and different grating periods(w_1 = 60nm,w_2 = 50nm, L_c = 2d_1 = 2d_2, N = 10).

4. Conclusion

In summary, a compact and high sensitive refractive index sensor based on the MIM plasmonic Bragg grating has been proposed. The refractive index sensing characteristics of the device was analyzed in detail and very good linear relationship between the Bragg

#223182 - $15.00 USD Received 15 Sep 2014; revised 19 Oct 2014; accepted 25 Oct 2014; published 10 Nov 2014

resonance wavelength and the refractive index was obtained. And by introducing a nano-cavity in the uniform MIM plasmonic Bragg grating structure, a high refractive index sensitivity of 1488nm/RIU and large FOM of about 20 around the resonance wavelength of 1550nm was obtained. Also the results show that the sensitivity of the proposed refractive index sensor can be increased by increasing the resonance wavelength, which can be easily realized by increasing the grating period. The proposed MIM plasmonic Bragg grating refractive index sensor has the merits of compact size (nanometric), high sensitive, linear response, large sensing range and relative high FOM, which makes it very promising for integrated chemical and biological sensing applications.

Acknowledgment

This work was supported by the National Science Foundation of China under Grant No.60907025, No.11374048 and the Fundamental Research Funds for the Central Universities.

#223182 - $15.00 USD Received 15 Sep 2014; revised 19 Oct 2014; accepted 25 Oct 2014; published 10 Nov 2014